Acta Biomaterialia 10 (2014) 2024–2035

Contents lists available at ScienceDirect

Acta Biomaterialia

journal homepage: www.elsevier.com/locate/actabiomat

Self-assembled pH-responsive hyaluronic acid–g-poly(L-histidine) copolymer micelles for targeted intracellular delivery of doxorubicin

Lipeng Qiu [a], Zhen Li [b], Mingxi Qiao [a], Miaomiao Long [a], Mingyue Wang [a], Xiaojun Zhang [a], Chenmin Tian [c], Dawei Chen [a,c,*]

[a] School of Pharmacy, Shenyang Pharmaceutical University, Shenyang 110016, People's Republic of China
[b] School of Pharmacy, Dalian Medical University, Dalian 116044, People's Republic of China
[c] College of Pharmaceutical Science, Soochow University, Suzhou 215123, People's Republic of China

ARTICLE INFO

Article history:
Received 2 August 2013
Received in revised form 5 December 2013
Accepted 13 December 2013
Available online 21 December 2013

Keywords:
Hyaluronic acid–g-poly(L-histidine)
Self-assembled micelles
pH-responsive
Targeted intracellular delivery
Doxorubicin

ABSTRACT

Hyaluronic acid (HA) was conjugated with hydrophobic poly(L-histidine) (PHis) to prepare a pH-responsive and tumor-targeted copolymer, hyaluronic acid–g-poly(L-histidine) (HA-PHis), for use as a carrier for anti-cancer drugs. The effect of the degree of substitution (DS) on the pH-responsive behaviour of HA-PHis copolymer micelles was confirmed by studies of particles of different sizes. In vitro drug release studies demonstrated that doxorubicin (DOX) was released from HA-PHis micelles in a pH-dependent manner. In vitro cytotoxicity assays showed that all the blank micelles were nontoxic. However, MTT assay against Michigan Cancer Foundation-7 (MCF-7) cells (overexpressed CD44 receptors) showed that DOX-loaded micelles with a low PHis DS were highly cytotoxic. Cellular uptake experiments revealed that these pH-responsive HA-PHis micelles taken up in great amounts by receptor-mediated endocytosis and DOX were efficiently delivered into cytosol. Moreover, micelles with the lowest DS exhibited the highest degree of cellular uptake, which indicated that the micelles were internalized into cells via CD44 receptor-mediated endocytosis and the carboxylic groups of HA are the active binding sites for CD44 receptors. Endocytosis inhibition experiments and confocal images demonstrated that HA-PHis micelles were internalized into cells mainly via clathrin-mediated endocytosis and delivered to lysosomes, triggering release of DOX into the cytoplasm. These results confirm that the biocompatible pH-responsive HA-PHis micelles are a promising nanosystem for the intracellular targeted delivery of DOX.

1. Introduction

The past decade has witnessed a development in tumor-targeted nanocarrier delivery systems for improving the efficacy of cytotoxic anticancer drugs [1–4]. Polymer micelles have been widely investigated as excellent carriers because of their self-assembled small size under aqueous conditions and their possession of targeting properties based on the enhanced permeability and retention (EPR) effect [5–8]. Intracellular delivery has been further improved by developing targeted and stimuli-responsive micelles. A variety of different approaches have been developed to allow conjugation of tumor-interacting moieties, such as antibodies [9], folic acid [10] and various other ligands [11,12] on the surface of micelles. However, the tumor-targeted moieties usually need extra modification which could affect their stability and targeting efficacy in vivo.

In recent years, hyaluronic acid (HA) has been widely investigated for use in tumor-targeted delivery because of its ability to specifically bind to various cancer cells [13,14]. HA is a biodegradable polyanionic polysaccharide with low toxicity, which is distributed widely in the extracellular matrix and connective tissues. Moreover, HA itself is a ligand for CD44 hyaluronan receptors, which are overexpressed in a variety of tumor types [15–17]. Based on these factors, a number of hydrophobic agents, such as ceramide [18], all-*trans* retinoid acid [19] and 5β-cholanic acids [20], have been conjugated to HA to produce novel targeting carriers for anti-tumor drug delivery to increase cellular uptake via CD44 receptor-mediated endocytosis. However, the intracellular drug release of the new nanocarriers plays an important role in tumor therapy and these HA-based micelles are unable to control the release of encapsulated drugs in tumor cells. Therefore, environmental stimuli-responsive micelle materials which are able to release entrapped drugs under the appropriate stimulus (such as pH,

* Corresponding author at: School of Pharmacy, Shenyang Pharmaceutical University, Shenyang 110016, People's Republic of China. Tel./fax: +86 24 23986306.
E-mail address: chendawei@syphu.edu.cn (D. Chen).

http://dx.doi.org/10.1016/j.actbio.2013.12.025
1742-7061/

temperature and magnetic field.) have recently attracted much attention [21–23]. Zhang and co-workers have exploited cystamine as a bioreducible linkage for the preparation of redox-sensitive hyaluronic acid–deoxycholic acid (HA-ss-DOCA) micelles. In particular, they found that paclitaxel-loaded HA-ss-DOCA micelles were much more cytotoxic than insensitive HA-DOCA micelles [24]. Although the HA-ss-DOCA carrier has some advantages for drug delivery, it requires a disulfide bond in linkages and the glutathione (GSH) responsive micelle degradation depends on a high level of GSH. However, the pH-responsive system is independent of the cellular chemical substances and does not require the exact location of tumors for triggered release compared with other stimuli-responsive strategies [22,25].

It is well known that the physiological pH in cancer cells is lower than that in blood and normal tissues, and is about 6.0 and 5.0 in intracellular early lysosomes and late lysosomes, respectively [26,27]. Hence, the acid-triggered rapid release of drugs can be achieved inside tumor cells by using micelles of copolymers bearing pH-responsive blocks, such as poly(L-histidine) (PHis) [28,29]. PHis has attracted substantial interest in studies of pH-responsive actuators due to its biodegradable, biocompatible and amphoteric nature [30]. After internalization, the PHis-based copolymer micelles are destabilized in lysosomes by pH-induced protonation of the imidazole ring, followed by lysosomal membrane disruption and release of the incorporated drug into the cytoplasm [31,32]. Therefore, hydrophobic PHis can be grafted onto hydrophilic HA for the development of targeted and pH-responsive micelles without any additional linkages. pH-Responsive HA-based micelles will be able to increase receptor-mediated accumulation at the tumor site followed by a burst of encapsulated drug release, providing an effective approach for the rapid transport of the drug cargo into the cytosol and significantly increase the antitumor efficacy. Furthermore, it has been reported that HA is degraded by hyaluronidases in lysosomal acidic condition [33]. Hence, when the pH-sensitive HA-based micelles encounter lysosomes, the acidic environment will sensitize the hyaluronidase action, resulting in a sustained cellular uptake of more new HA micelles [34].

The most important advantage of this novel design is that the pH-responsive HA-based micellar delivery system with smart functions such as active targeting and pH-triggered drug release provides an effective approach for increasing cellular uptake and rapid delivery of the cargo drug into the cytosol, resulting in significant increases in therapeutic efficacy. In this study, an amphiphilic HA-PHis copolymer with native targeting and pH-responsive features was synthesized by conjugation of HA with PHis oligomer. Different degrees of substitution (DS) of HA-PHis copolymers were used to investigate the influence of the DS of PHis on the targeting of CD44 receptors because the recognition sites of CD44 receptors might be the carboxylic groups of HA [35]. Copolymer micelles based on HA-PHis were developed for targeted and intracellular delivery of doxorubicin (DOX), an effective anticancer drug. As shown in Scheme 1, HA-PHis copolymers self-assemble into micelles under aqueous conditions and accumulate at the tumor site by the EPR effect. Then, the micelles can be selectively taken up and internalized into the tumor cells via CD44 receptor-mediated endocytosis and transported to lysosomes, where the micelles disassemble rapidly due to pH-induced protonation of PHis, followed by lysosomal membrane disruption and cytoplasm drug burst release. The physical characteristics and drug-loading capacities of the micelles were studied in detail and the pH-sensitivity of the micelles was characterized by the size distribution change and in vitro drug release in different pH environments. In addition, the cytotoxicity of blank and DOX-loaded micelles and the receptor-mediated targeting effect of micelles based on different DS of HA-PHis copolymers were evaluated. The internalization mechanism and intracellular drug release of the HA-PHis micelles in MCF-7 cells were also studied in the presence of endocytosis inhibitors by confocal microscopy.

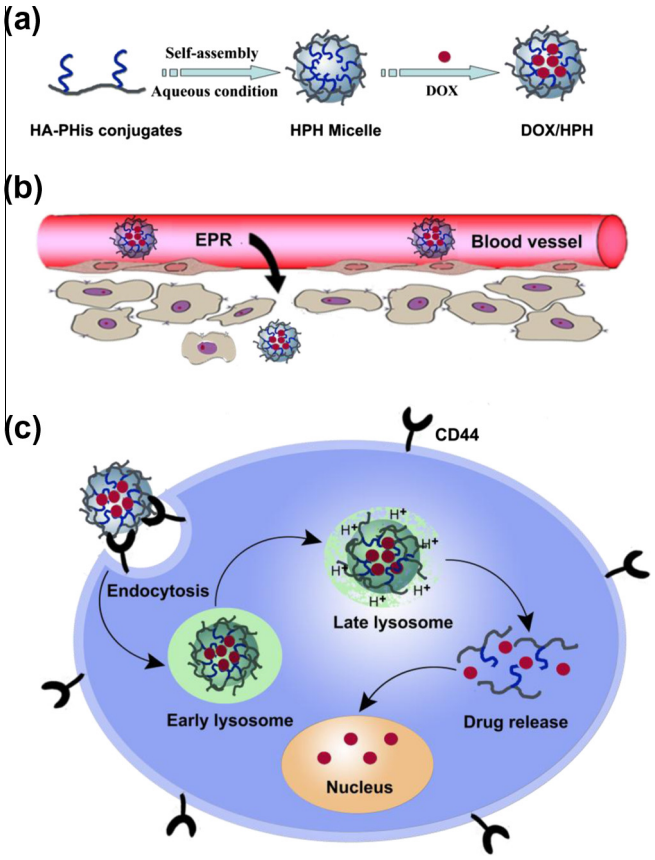

Scheme 1. Schematic illustration of self-assembly HA-PHis micelles and pH-responsive intracellular drug delivery. (a) The DOX-encapsulated micelles based on HA-PHis copolymers are formed in aqueous condition. (b) Particles of suitable size promote nanocarrier accumulation in tumor tissue by the EPR effect. (c) The micelles are selectively taken up by tumor cells via CD44 receptor-mediated endocytosis and delivered to the lysosomes, triggering the release of DOX into the cytoplasm, improving intracellular drug release and increasing the antitumor efficacy.

2. Experimental section

2.1. Materials

Sodium hyaluronate (Mw = 11 kDa) was purchased from Shandong Freda Biopharm Co. Ltd. (Shandong, PR China). N^{α}-CBZ-N^{im}-DNP-L-histidine was purchased from GL Biochem Co. Ltd. (Shanghai, PR China). *N*-Hydroxysuccinimide (NHS) and 1-ethyl-3-(3-dimethylaminopropyl) carbodiimide (EDC) were obtained from Sinopharm Chemical Reagent Co. Ltd. (Shanghai, PR China). Pyrene was supplied by Sigma-Aldrich Co. (St Louis, MO, USA). Doxorubicin hydrochloride was purchased from Beijing Huafeng United Technology Co. Ltd. (Beijing, PR China) and 3-(4,5-dimethylthiazol-2-yl)-2,5-diphenyl tetrazolium bromide (MTT), Hoechst 33342 and Lysotracker Green NDN-26 were obtained from Shanghai Beyotime Biotechnology Co. Ltd. (Suzhou, PR China). Chlorpromazine (CPM), chloroquine diphosphate (CQ) and colchicine (CC) were purchased from Shanghai Genestar Co. Ltd. (Shanghai, PR China). Filipin (FLP) was from the Cayman Chemical Company (Ann Arbor, MI, USA). Dulbecco's modied Eagle medium (DMEM), fetal bovine serum (FBS) and penicillin–streptomycin solution were purchased from Gibco BRL (Bethesda, MD, USA). All other chemicals were of analytical grade.

2.2. Synthesis of HA-PHis copolymers

Poly(N^{im}-DNP-L-histidine) (PHis-DNP) was prepared by ring-opening polymerization of protected L-histidine N^{im}-carboxyanhydride with isopropylamine initiator, as described by Lee et al. with minor modification [30]. HA was hydrophobically modified by chemical conjugation of PHis through amide formation. HA (0.26 mmol, moles of the carboxyl group) was dissolved in 10 ml anhydrous formylamine at 40 °C. After the solution was cooled to room temperature, EDC (0.52 mmol) and NHS (0.52 mmol) were added and the mixture was stirred for 2 h in an ice bath to activate the carboxylic group of sodium hyaluronate. Then, different amounts of PHis-DNP (0.13–0.52 mmol, the molar ratios between the carboxyl group of HA and the amino group of PHis were 2:1, 1:1 and 1:2) dissolved in anhydrous *N*,*N*-dimethylformamide were added slowly to the HA solution. The reaction mixture was stirred for 6 h at 50 °C and for another 40 h at room temperature under a nitrogen atmosphere. The resulting solution was dialyzed against an excess of water/ethanol (1:3-1:1, v/v) for 1 day and distilled water for 2 days [20,36]. After filtration, the solution was freeze-dried to obtain HA-PHis-DNP powder.

HA-PHis-DNP was dissolved in 5 ml formylamine and β-mercaptoethanol was added. The mixture was stirred for 24 h at 30 °C under a nitrogen atmosphere and then the solution was dialyzed against distilled water for 3 days, followed by lyophilization. The obtained copolymer HA-PHis was characterized by ^{1}H nuclear magnetic resonance (NMR) spectrometry (400 Hz, Varian, USA).

2.3. Characterization of HA-PHis micelles

The critical micelle concentration (CMC) of HA-PHis copolymer was determined using a fluorescence spectrophotometer with pyrene as a hydrophobic probe [37]. Briefly, pyrene solution in acetone (6.0×10^{-5} M) was prepared and the acetone was then evaporated completely under a gentle nitrogen gas stream for 1 h at 60 °C. HA-PHis solutions with concentrations ranging from 5.0×10^{-4} to 2.0 mg ml^{-1} were added to each tube to achieve a final pyrene concentration of 6.0×10^{-7} M. Then, these solutions were heated at 45 °C for 3 h and kept at room temperature overnight. Pyrene fluorescence spectra were obtained using a fluorescence spectrophotometer (LS55, PerkinElmer, USA). Excitation was carried out at 336 nm and the emission was recorded over the range 360–450 nm. The intensity ratio of the first peak (I_1, 373 nm) to the third peak (I_3, 384 nm) was analyzed to calculate the CMC.

The hemolytic activity of HA-PHis was investigated using rabbit red blood cells (RBCs) [38]. Surfactants, including Tween 80 and soybean phospholipid (SP), were used as controls. After collection, the RBCs were centrifuged at 1500 rpm for 10 min and washed three times with normal saline to harvest the erythrocytes. The cell pellets were resuspended in saline to obtain a 2% suspension (v/v) and the erythrocytes were used within 24 h. An RBC suspension (0.5 ml) was added to 0.5 ml copolymer samples until the final concentrations of HA-PHis, Tween 80 and SP ranged from 0.1 to 4 mg ml^{-1}. The mixture was incubated at 37 °C for 2 h and then centrifuged at 5000 rpm for 5 min to remove intact RBCs. The supernatant was collected and the released hemoglobin was determined using a UV-2600 spectrophotometer (Shimadzu, Japan) at 570 nm. To obtain 0 and 100% hemolysis, 0.5 ml normal saline and 0.5 ml distilled water was added to 0.5 ml RBC suspension, respectively. All measurements were performed in triplicate and the degree of hemolysis was calculated using the following equation:

$$\text{Hemolysis } (\%) = \frac{A_s - A_0}{A_{100} - A_0} \times 100, \quad (1)$$

where A_s, A_{100} and A_0 are the absorbance of samples, a solution of 100% hemolysis and a solution of 0% hemolysis, respectively.

The stability of HA-PHis copolymer micelles in the presence of DMEM with FBS was determined by dynamic light scattering spectrophotometry (PSS·Nicomp, Santa Barrara, USA), as described by Choi et al. with some modification [39]. Different DS of micelles in phosphate-buffered saline (PBS, 1 mg ml^{-1}) were mixed with an equal volume of DMEM containing 10% FBS. The mixture was kept in a shaking rocker at 100 rpm and 37 °C and particle size measurements were obtained at different times; the experiment was repeated for three different samples.

2.4. pH-Responsive behaviour of HA-PHis micelles

HA-PHis was dissolved in PBS at pH 8.0 to obtain a concentration of 1.0 mg ml^{-1}. Then, 10.0 ml of the micelle solution was taken and its pH was adjusted from pH 8.0 to 4.0 with hydrochloric acid and the changes in the particle size were examined by dynamic light scattering spectrophotometry (PSS·Nicomp). All the operations were carried out according to the Nicomp ZLS User Manual. Before determination, 100 μl of the micelle solution was diluted with 3.0 ml distilled water in order to keep the intensity value on the front panel of the instrument at approximately 300 kHz, which is recommended for a sample that scatters effectively. All measurements were performed in triplicate.

2.5. Preparation and characterization of DOX-loaded HA-PHis micelles

DOX·HCl (100 mg, 0.17 mmol) was dissolved in 4 ml methanol/acetone (1:1, v/v) and 50 μl triethylamine (35 mg, 0.35 mmoL) was added. After 12 h of stirring at room temperature, the solution was subjected to rotary evaporation at 40 °C and freeze-dried to obtain the base form of DOX. DOX-loaded copolymer micelles were prepared by the probe-type ultrasonication technique in which 10 mg HA-PHis copolymer was dispersed in 10 ml PBS (0.1 M, pH 8.0) and 2 mg DOX was dissolved in tetrahydrofuran/acetone (1:1, v/v). Then, the DOX solution was injected into the copolymer solution slowly with stirring at room temperature. The mixture was ultrasonicated for 30 min (carried out every 2 s for a 3 s duration with an output power of 100 W, JY92-II, Xinzhi Scientific Instrument Institute Co. Ltd., PR China) in an ice bath after stirring at room temperature for least 24 h to remove the solvent. The final micellar dispersion was passed through a 0.45 μm microfiltration membrane to remove insoluble drug.

The particle size, polydispersity and zeta potential of the micelles were assessed using a Nicomp™ 380ZLS (PSS·Nicomp) as described in Section 2.4. The morphology of the micelles was observed by transmission electron microscopy (TEM; Tecnai G220, FEI, USA). Before visualization, the micelle suspensions were placed on copper grids with films, air-dried for 10 min and finally examined by TEM.

For measurement of the drug loading (DL) and encapsulation efficiency (EE), 0.5 ml DOX-loaded micellar solution was mixed with 9.5 ml formylamine, and disrupted by ultrasonic treatment in a water bath for 10 min. The DOX concentration was measured using a UV spectrophotometer (UV-2600, Shimadzu, Japan) at 479 nm. Empty micelles of HA-PHis copolymers were prepared as a blank and the DL and EE were calculated as the ratio of the drug weight in the micelles to the total weight of the micelles and feeding weight of drug, respectively. All measurements were performed in triplicate.

2.6. In vitro release of DOX from HA-PHis micelles

The release profiles of DOX from the micelles were investigated using a dialysis bag (molecular weight cutoff 3500 Da) at 37 °C.

Briefly, a dialysis bag with 2.0 ml DOX-loaded micelles was immersed in 20 ml fresh PBS solution (pH 5.0 and 7.4, 0.1 M) in a vial, which was placed in a shaking incubator at a stirring speed of 100 rpm at 37 °C. At predetermined intervals, 1.0 ml samples were taken and replaced by the same volume of fresh buffer to maintain the total volume. The concentration of DOX released into PBS was measured with a UV–visible spectrophotometer as described previously. The cumulative percentage drug release (Er) was calculated as follows:

$$\mathrm{Er}\ (\%) = \frac{V_e \sum_1^{n-1} C_i + V_0 C_n}{m_{DOX}} \times 100, \quad (2)$$

where m_{DOX} represents the amount of DOX in the micelles, V_0 is the whole volume of the release medium, and C_i represents the concentration of DOX in the *i*th sample. The in vitro release experiments were carried out in triplicate at each pH.

2.7. In vitro cytotoxicity assays

The cytotoxicity of blank HA-PHis micelles and DOX-loaded HA-PHis micelles against Michigan Cancer Foundation-7 (MCF-7) cells was evaluated by the standard MTT assay [40]. Briefly, the cells were seeded at a density of 5×10^3 cells per well in 96-well plates and incubated for 24 h to allow cell attachment. The cells were then incubated with free DOX, blank micelles and DOX-loaded micelles in a concentration gradient at 37 °C. After 48 h incubation, 10 μl MTT (5 mg ml^{-1}) was added to the medium and further incubated for 4 h. The medium in each well was removed and 100 μl DMSO was added to dissolve the internalized purple formazan crystals. The absorbance at 492 nm was recorded using a BioRed microplate reader (MK3, Thermo, USA). The relative cell viability (%) was calculated using the following equation:

$$\text{Cell viability}\ (\%) = \frac{A_{sample} - A_{blank}}{A_{control} - A_{blank}} \times 100, \quad (3)$$

where $A_{control}$ and A_{sample} are the absorbance in the absence and in the presence of sample treatment, respectively. A_{blank} is the absorbance of the medium. The IC_{50} values of different groups were then calculated using SPSS 17.0 (Chicago, IL, USA). All measurements were performed in triplicate.

2.8. Cellular uptake

The cellular uptake and cellular distribution of HA-PHis micelles were observed by fluorescence microscopy (IX51, Olympus, Japan). MCF-7 cells were seeded in 24-well plates at a density of 1×10^4 cells per well and incubated for 48 h at 37 °C. Free DOX or DOX-loaded micelles (5.0 μg ml^{-1} of DOX) in serum-free medium was added and incubated for 0.5, 1 and 2 h. After incubation, all reagents were removed and Hoechst 33342 (10 μg ml^{-1}, 15 min) was used to visualize the nuclei. Afterwards, cells were viewed by fluorescence microscopy.

The cellular uptake of micelles was also analyzed quantitatively using flow cytometry. MCF-7 cells were seeded at a density of 2×10^4 cells per well in 6-well plates and incubated for 24 h. After incubating with free DOX and DOX-loaded micelles (5.0 μg ml^{-1} of DOX) for 0.5, 1 and 2 h, the cells were washed three times with cold PBS (pH 7.4), harvested and subsequently resuspended in 0.5 ml PBS for flow cytometrix analysis (FC500, Beckman Coulter, USA). All measurements were performed in triplicate.

2.9. Endocytosis inhibition

To study the effect of different inhibitors on the uptake of HA-PHis micelles, cells were pre-incubated individually with the following inhibitors: 10 μg ml^{-1} CPM, 40 μg ml^{-1} CC, 5 μg ml^{-1} FLP and 10 mg ml^{-1} HA [36,41]. After pre-incubation for 30 min, HPHM-19 containing 5 μg ml^{-1} DOX was added and incubated for a further 2 h. Subsequently, cells were washed and harvested for analysis using the methods described in Section 2.8. All measurements were performed in triplicate.

2.10. Intracellular release of DOX

Laser scanning confocal microscopy (LSCM) was used to visualize the subcellular localization and intracellular release behavior of HPHM-19 [42]. MCF-7 cells were cultured on microscope slides in a 6-well plate (1×10^4 cells per well) and incubated for 24 h. Then HPHM-19 (5 μg ml^{-1} DOX) was added and the cells were incubated further for 10, 30, 60 and 120 min at 37 °C. Then, the medium was removed and Lysotracker Green (80 μg ml^{-1}, 60 min) and Hoechst 33342 (10 μg ml^{-1}, 15 min) were used to visualize the lysosomes and nuclei, respectively. Finally, the cells were treated with 5% paraformaldehyde at room temperature for 15 min and images were obtained by LSCM (TCS-SP2, Leica, Germany). In order to study the effect of the lysosomal pH on the drug release of micelles, chloroquine (8 μg ml^{-1}) was added 1 h before the addition of HPHM-19.

2.11. Statistical analysis

All experiments were performed in triplicate and the data were presented as mean ± standard deviation (SD). One-way ANOVA with Student–Newman–Keuls post hoc test was performed to evaluate the difference among the groups and *P*-values < 0.05 were considered statistically significant.

3. Results and discussion

3.1. Synthesis and characterization of HA-PHis copolymers

The HA-PHis copolymer was synthesized by grafting the carboxyl group of HA on to an amino group of PHis in the presence of EDC and NHS, as shown in Scheme 2. In this investigation, HA can be used as a tumor-targeting moiety and PHis was conjugated with HA as a hydrophobic group to make it pH responsive. The peaks for the *N*-acetyl group (1.91 ppm) of HA, the isopropylamine methyl group (1.07 and 1.21 ppm) and the imidazole ring of PHis (7.18 and 8.47 ppm) were confirmed by the ^{1}H NMR spectrum, indicating that HA-PHis had been successfully synthesized (Fig. 1).

The DS, defined as the number of PHis groups per 100 sugar residues of HA copolymer, was controlled by varying the molar ratio of the carboxyl group of HA to the amino group of PHis. The DS was determined by calculating the relative intensity ratio between the *N*-acetyl peak in HA and the methyl peaks in PHis in the ^{1}H NMR spectrum of HA-Phis [18]. An interesting result was that when the molar ratio of the carboxyl group of HA to the amino group of PHis was 2:1, 1:1 and 1:2, the DS of PHis was 28%, 19% and 22%, and these were named HPH-28, HPH-19 and HPH-22, respectively. It is possible that HA became twisted in the reaction solution, thus shielding the carboxyl group. Hence, the amino group could react fully with the carboxyl group at a molar ratio 2:1 to obtain the highest DS. When the ratio increased to 1:1, the competition and intermolecular interactions of the amino group were increased, resulting in a lower DS. However, the ratio continued to increase to 1:2, and there were many amino groups remaining in solution, which increased the reaction efficiency with a higher DS.

The CMC is an important parameter affecting the aggregation behavior of copolymer micelles in solution, and this involves the

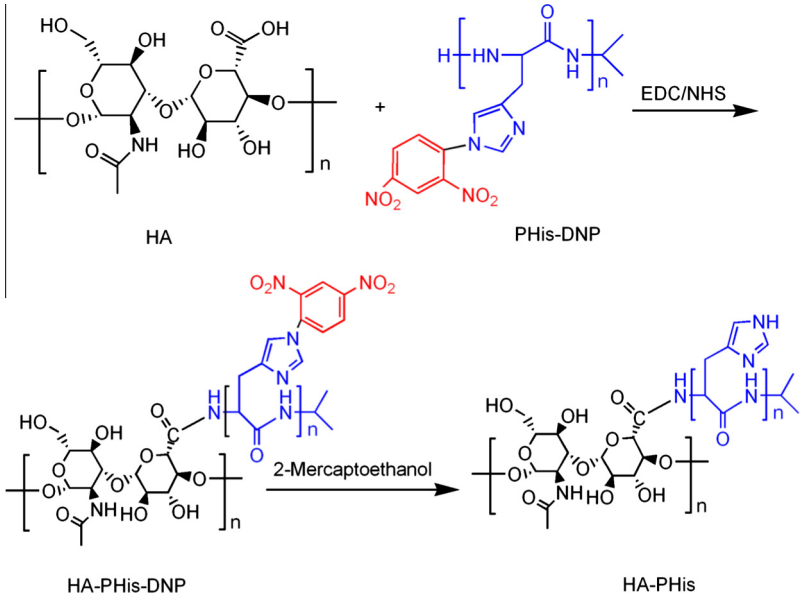

Scheme 2. Synthesis of HA-PHis copolymers.

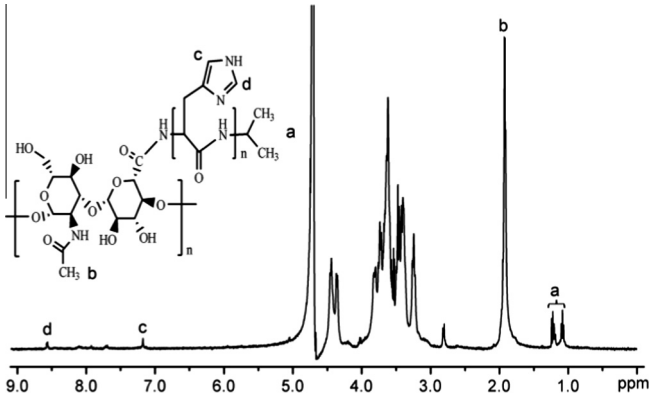

Fig. 1. ^{1}H NMR spectrum of HA-PHis copolymers.

self-assembly ability of the amphiphilic copolymer and the structural stability of micelles in vitro and in vivo [36]. The CMC values of HA-PHis with different DS were studied by fluorescence spectroscopy using pyrene as a hydrophobic fluorescence probe. In Fig. 2a, the fluorescence intensity ratio (I_{373}/I_{383}, I_1/I_3) derived from the HA-PHis concentration was plotted and the CMC was estimated from the threshold concentration of the self-assembled nanoparticles. The CMC values of HA-PHis copolymers ranged from 20.4 to 45.7 μg ml^{-1}—significantly lower than those of other low molecular weight surfactants [18]. This low CMC value indicates that a better structural integrity can be produced at a low copolymer concentration even under extreme dilution. This may maintain the stability of micelles in the bloodstream after intravenous administration. Moreover, the CMC of the HA-PHis copolymers decreased as the DS of the hydrophobic groups increased, because the higher hydrophobicity renders the formed micelles more compact, which then results in a lower CMC.

The amphiphilic copolymers appear to have similar properties to surfactants, such as causing cell membrane damage [43]. Therefore, a hemolysis assay was performed in order to estimate the biocompatibility of the HA-PHis copolymer micelles. The level of hemolysis of HA-PHis was compared with that of Tween 80 and SP, which are typical surfactants used for i.v. administration. The degree of hemolysis at different concentrations of HA-PHis, Tween 80 and SP are shown in Fig. 2b. As the concentration increased, the hemolysis induced by Tween 80 and SP increased dramatically. At a concentration of 1 mg ml^{-1}, the hemolysis caused by Tween 80 and SP reached 47.6 ± 2.53% and 60.9 ± 2.91%, respectively, while HPH-19, HPH-22 and HPH-28 were all basically nonhemolytic, exhibiting no more than 2.0% hemolysis even at 4 mg ml^{-1}, which was significantly different from Tween 80 and SP ($P < 0.05$). In addition, no significant difference was observed among the HA-PHis with different DS values ($P > 0.05$). These results from the hemolysis experiments demonstrated that HA-PHis copolymers did not show significant hemolysis of RBCs in vitro.

The interaction of serum proteins with the copolymer micelles is one of the main reasons for the change in their properties in vivo [39,44]. The stability of HA-PHis copolymer micelles in the presence of complete medium with FBS at 37 °C was therefore investigated. As shown in Fig. 2c, the different micelles were relatively stable after incubation in FBS for 72 h, indicating that only a small amount of serum protein had become adsorbed on the micelles. The remarkably stability, which is important for applications in vivo, might have arisen by the production of a hydrophilic anionic shell layer in a serum environment.

The pH-responsive feature introduced by PHis in HA-PHis copolymer was measured in terms of the size change at different pH values (Fig. 3). The average particle diameter remained almost unchanged at pH > 6.5 and it was confirmed that these copolymer micelles had a narrow particle diameter distribution. Stepwise shifts in the pH of the solution to lower pH values resulted in a sudden increase in average size between pH 6.0 and 5.0, while the particle diameter distribution increased with a standard deviation of >10% at pH < 6.5. This pH-dependent behaviour was induced by the ionizable imidazole group: more imidazole groups are protonated under more acidic conditions, leading to dissociation of the micelles and an increase in the average size.

3.2. Formation and characterization of DOX-loaded HA-PHis micelles

Self-assembled HA-PHis micelles were prepared using a simple ultrasonic method without adding stabilizer, emulsifier or other agents. It was likely that grafted hydrophobic PHis chains are clustered in the micelle core, while the hydrophilic backbone of HA serves as the shell for the copolymer micelles in aqueous solution, as shown in Scheme 1a. DOX was physically incorporated into HPH-19, HPH-22 and HPH-28 copolymers, which were named

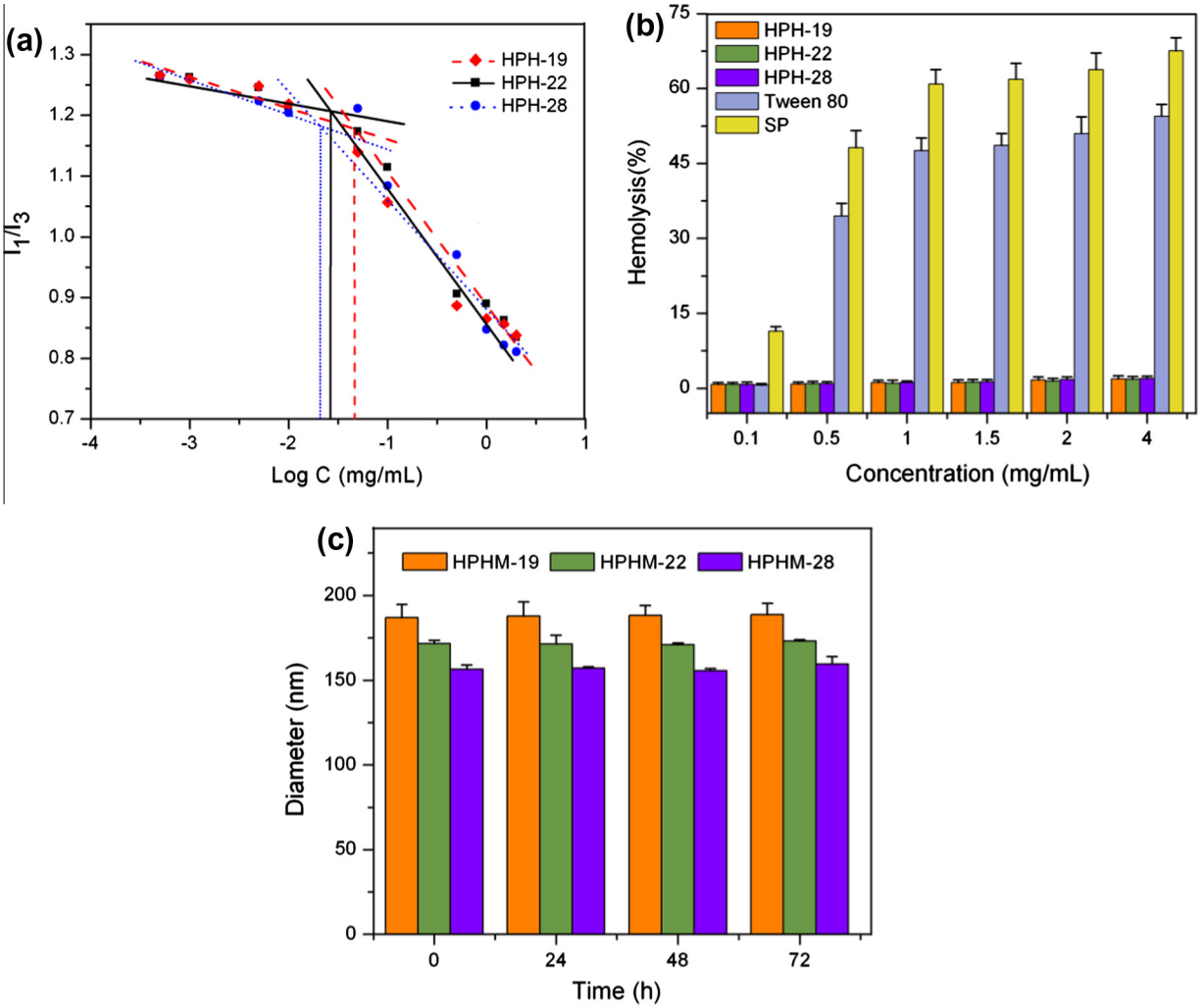

Fig. 2. Characterization of HA-PHis copolymer micelles: (a) CMC determination, (b) hemolysis assay and (c) stability analysis in the presence of FBS at 37 °C ($n = 3$).

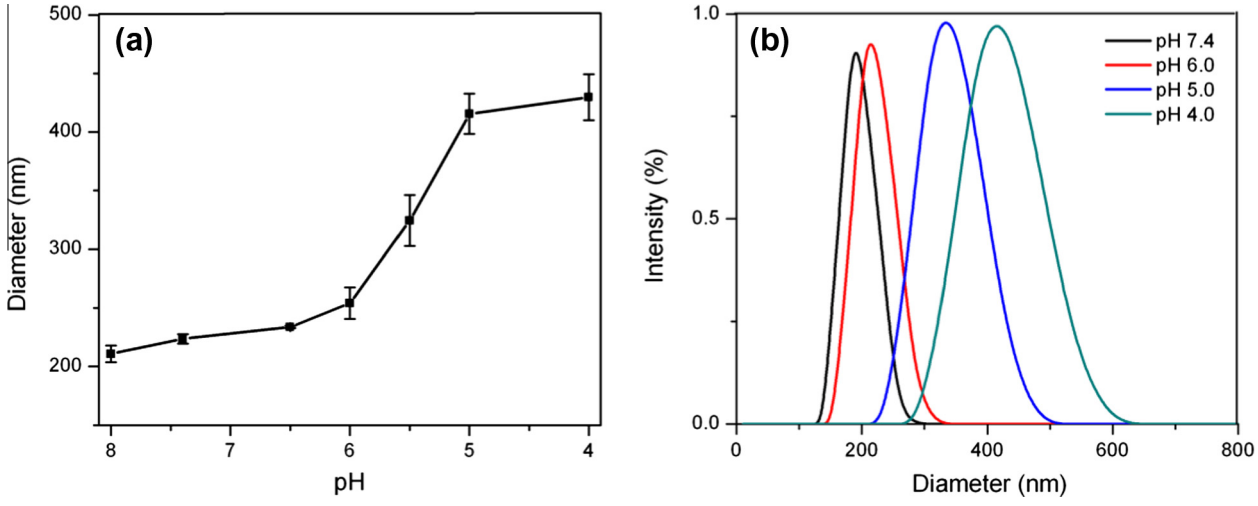

Fig. 3. Particle diameter distribution of HPH-19 at different pH values at 37 °C ($n = 3$).

HPHM-19, HPHM-22 and HPHM-28, respectively. The average particle sizes, polydispersity index (PDI), zeta potentials, EE and DL of the DOX-loaded micelles are summarized in Table 1. It was found that HA-PHis copolymers formed monodisperse micelles with a low PDI and the average sizes and zeta potentials of the HA-PHis micelles changed as the DS values increased. This was probably due to the hydrophobic strength of the micellar core packing and the reduction in the carboxyl groups of HA-PHis, resulting in a decrease in both the size and surface charge. Meanwhile, the modest negative zeta potentials indicated that the micellar surface was covered by the negatively charged HA polymers, which would prevent the aggregation of micelles through electrostatic repulsion.

Table 1
Characterization of DOX-loaded HA-PHis micelles.

	Size (nm)	PDI	Zeta (mV)	EE[a] (%)	LC[b] (%)
HPHM-19	215.7 ± 3.3	0.120 ± 0.04	−10.7 ± 0.94	90.7 ± 2.4	6.77 ± 0.38
HPHM-22	173.3 ± 1.4	0.233 ± 0.02	−9.83 ± 0.70	87.2 ± 1.9	6.06 ± 0.16
HPHM-28	154.8 ± 1.6	0.152 ± 0.04	−7.29 ± 0.69	84.8 ± 2.1	4.23 ± 0.12

[a] EE (%) = encapsulation efficiency.
[b] LC (%) = drug loading content.

TEM micrographs showed that the micelles have a nearly spherical morphology, as shown in Fig. 4a. Compared with the determination by DLS, the smaller size was probably due to the difference in the two measuring methods. The shrinkage of the micellar shell during the TEM sample preparation process may have led to a decrease in the size of the micelles. In addition, DL and EE slightly decreased with an increase in the DS of PHis in HA-PHis micelles. A possible explanation for this finding is that the polymerization of PHis oligomers which gathered in the micellar core and the very strong hydrophobicity would result in a weak exclusion between the hydrophobic DOX and the micellar core region.

3.3. pH-Triggered release of DOX from HA-PHis micelles

The pH-dependent drug release behavior of the HA-PHis micelles was investigated at a physiological pH (7.4) and a lysosomal pH (5.0) at 37 °C, as shown in Fig. 4b. A significant difference was found in the DOX release at pH 7.4 and 5.0 ($P < 0.05$). DOX was slowly released from the micelles at pH 7.4 with no more than 40% release being achieved after 12 h. This suggested that DOX was released in a sustained manner and the DOX-loaded copolymer micelles maintained their micellar structures under physiological conditions (pH 7.4). In contrast, the DOX release rate was much faster at a lower pH (pH 5.0), with about 70% of DOX being released in 12 h. It was also noted that the drug release from HA-PHis micelles with three different DS were different even under the same pH conditions. The release data for HPHM-19 and HPHM-28 showed a significant difference ($P < 0.05$) at pH 5.0, which was most likely due to the different amounts of PHis in the micelle core. However, there were no significant differences ($P > 0.05$) among the other micelles either at pH 7.4 or 5.0. Therefore, it is clear that the pH-responsive ability of the DOX-loaded HA-PHis micelles is associated not only with superior stability in unwanted extracellular compartments but also with the rapid release of encapsulated DOX in the lysosomes of the target disease cells. This would ensure effective intracellular drug delivery and improve the bioavailability of DOX in tumor cells [22,45].

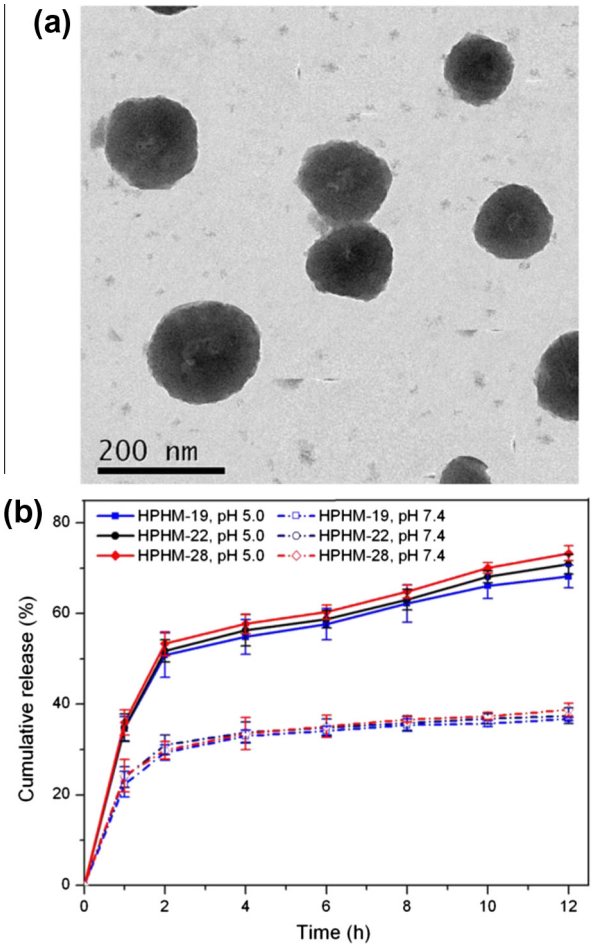

Fig. 4. (a) TEM images of HPHM-19 and (b) pH-dependent release of DOX from HA-PHis micelles at 37 °C ($n = 3$).

The mechanism of drug release from polymeric matrices is very complex and not completely understood [46]. Some nanoparticle drug delivery systems may be classified as either purely diffusion or degradation controlled [47], while others exhibit a combination of these mechanisms [48]. In this study, we hypothesized that the release of DOX from HA-PHis copolymer micelles into the solution medium may be determined by either micelle degradation or diffusion. The release behavior at different pH values was studied, and it was found that both the rate and the amount of DOX release increased with a reduction in pH. It might be that the micelles have compact PHis cores and the release of DOX from the cores is almost completely diffusion controlled at pH 7.4, which leads to a slow release rate. However, at pH 5.0, a gradual increase in the DOX polarity may be determined by a combination of diffusion through the polymer layer and degradation of the micelles, and the predominant mechanism may be degradation [46,49]. Furthermore, the accelerated micelle rate might be related to the swollen hydrophobic core which could cause the drug molecules close to the surface to diffuse into the medium [50]. Luo et al. reported that the drug release of pH-sensitive micelles follows a swelling–demicellization–releasing mechanism [51]. Because of ionization–deionization of the imidazole ring on the PHis block, its swelling behavior greatly depends on the pH. By maintaining the pH of the solution at 7.4, the micelles have unimpaired PHis cores and DOX is released slowly via a diffusion mechanism. On lowering the pH of the solution to 5.0, the PHis blocks are protonated and the charged imidazole groups repel each other, leading to marked swelling, and DOX gradually moves out. Finally, the PHis chains of the swollen micelles move out of the core, exposing them to a polar environment which leads to demicellization of the HA-PHis micelles [51–54]. Moreover, it has been reported that the stability of the DOX molecules is enhanced due their ionization in a low pH environment which results in an increased diffusion, inhibiting all nonbonding interactions with the copolymer walls [52].

3.4. In vitro cytotoxicity studies

The cell viability of HA-PHis-based blank micelles and DOX-loaded micelles against MCF-7 cells was evaluated. The cell viability of blank micelles was measured after a 48 h incubation. As shown in Fig. 5a, the empty micelles with different DS were nontoxic to MCF-7 cells and the viability was over 95% at all concentrations (50-800 mg ml^{-1}) tested. This indicated that all HA-PHis copolymer micelles were nontoxic and biocompatible and could be used as a delivery system for anticancer agents.

In addition, the enhanced cytotoxicity of DOX-loaded micelles and free DOX was observed along with an increase in their dose as shown in Fig. 5b. The IC_{50} values of each group were also calcu-

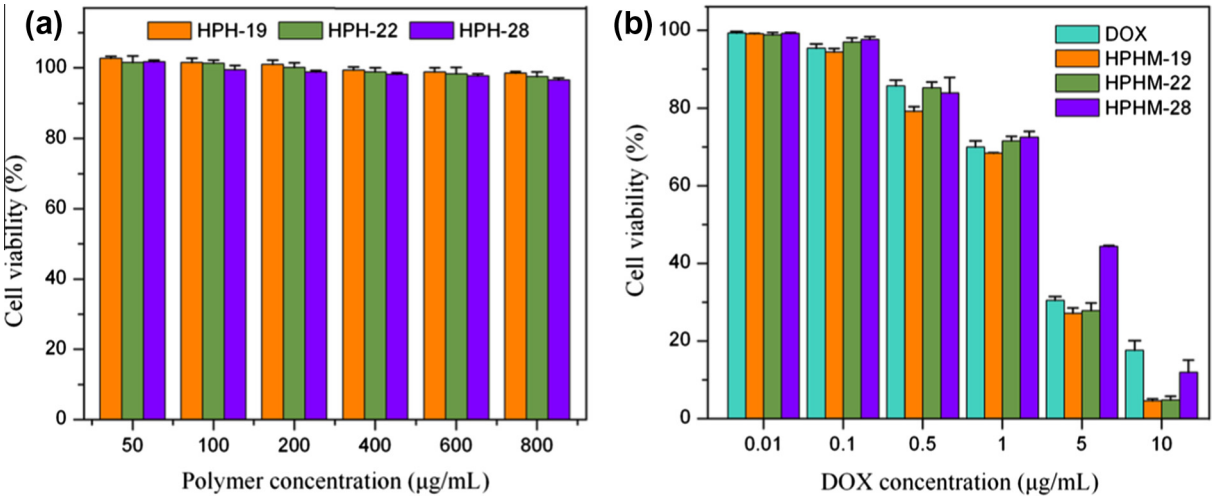

Fig. 5. In vitro cytotoxicity of (a) blank micelles and (b) DOX-loaded HA-PHis micelles and free DOX in MCF-7 cells ($n = 3$).

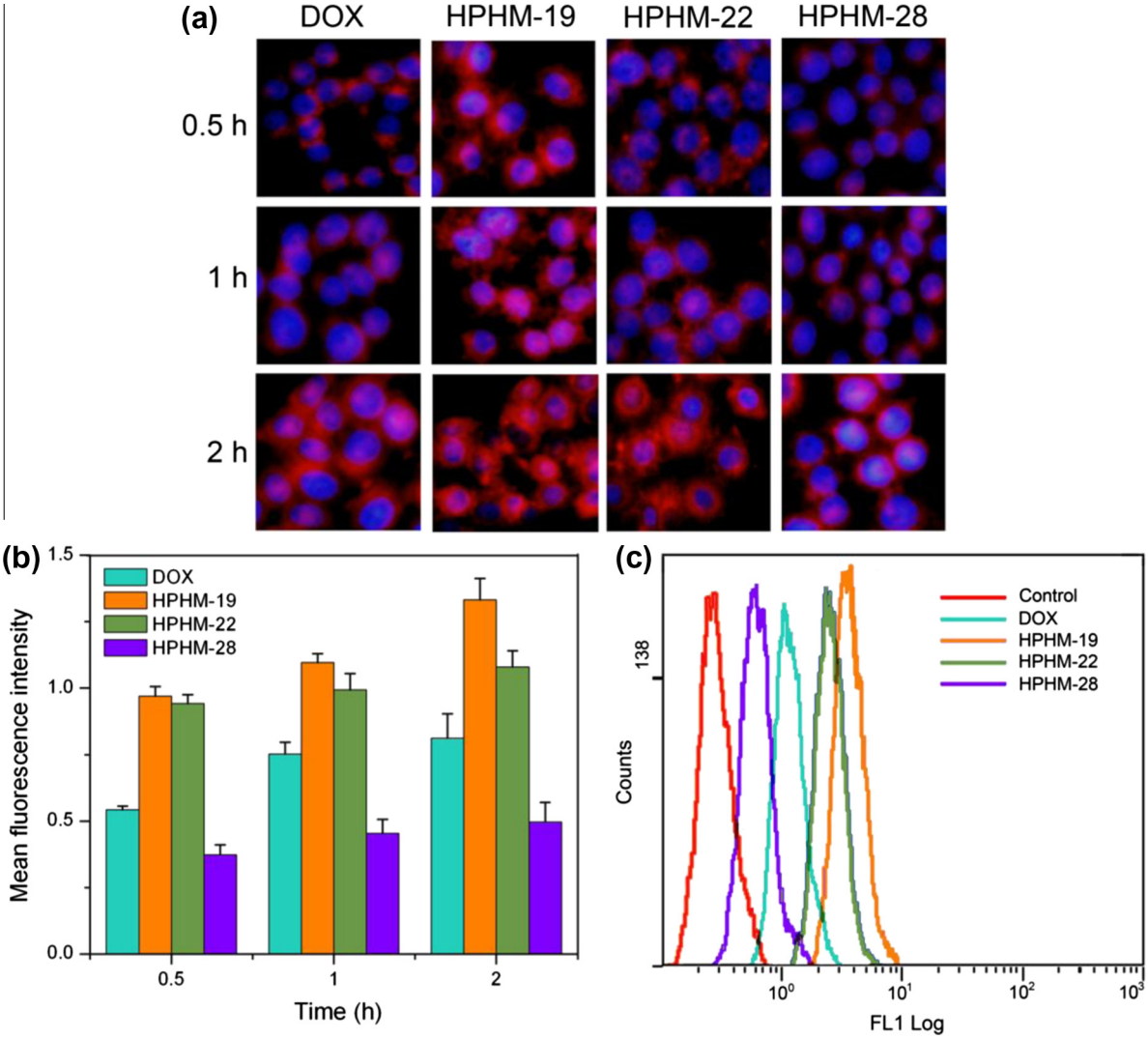

Fig. 6. (a) Fluorescence microscopy images of MCF-7 cells incubated with DOX-loaded HA-PHis micelles and free DOX. Blue and red colors indicate Hoechst 33342 and DOX, respectively. (b) Flow cytometry measurement of the intracellular uptake of DOX-loaded HA-PHis micelles and free DOX in MCF-7cells and (c) the fluorescence intensity of DOX accumulation at 2 h.

lated. It was worth noting that HPHM-19, HPHM-22 and HPHM-28 displayed differences in cell cytotoxicity in terms of both viabilities and IC_{50} values. As the DS of PHis increased, the IC_{50} values also increased. HPHM-19 had the lowest IC_{50} (1.76 ± 0.06 μg ml^{-1})

compared with HPHM-22 ($2.03 \pm 0.09\ \mu g\ ml^{-1}$) and HPHM-28 ($2.59 \pm 0.13\ \mu g\ ml^{-1}$), suggesting that the cytotoxicity of HPHM-19 was significantly higher than that of HPHM-22 and HPHM-28 ($P < 0.05$). The reason for this might be that the carboxylic groups of HA, an active site which can identify CD44 receptors on the surface of tumor cells, became more occupied as the DS increased. Therefore, HA-PHis micelles with a lower DS could be more efficiently taken up via receptor-mediated endocytosis and deliver more DOX into cells, resulting in increased cytotoxicity.

Interestingly, another result showed that the IC_{50} of free DOX ($2.38 \pm 0.05\ \mu g\ ml^{-1}$) was significantly higher than that of HPHM-19 and HPHM-22 ($P < 0.05$). Compared with passive diffusion of free DOX through the cell membrane, the higher cytotoxicity of HPHM-19 and HPHM-22 might be attributed to the fact that the higher binding affinity between HA derivatives and CD44 receptors resulted in a more effective uptake of copolymer micelles. Moreover, on entry into tumor cells, DOX-loaded HA-PHis micelles could escape quickly from lysosomes and rapidly release DOX into the cytoplasm because of the pH-responsive nature of PHis, which would enhance the cytotoxicity of HPHM-19 and HPHM-22. However, the free DOX with a lower IC_{50} was more efficient in terms of cancer cell inhibition than HPHM-28 ($P < 0.05$). This is also assisted by the reduction in the active sites of binding with CD44 receptors.

3.5. In vitro cellular uptake studies

To evaluate the intracellular uptake efficiency, fluorescence microscopy was used to identify the location of the DOX in MCF-7 cells. The fluorescence microscope images of MCF-7 cells after 0.5, 1 and 2 h of incubation with free DOX, HPHM-19, HPHM-22 and HPHM-28 are presented in Fig. 6a. For all the groups, DOX—marked by a weak fluorescence signal—was distributed mainly in the cytoplasm after 0.5 h incubation. Then, the intracellular DOX intensity was increased and some drug reached the nucleus after 1 h. However, the fluorescence intensity was markedly increased in the cytoplasm after 2 h and a large amount of DOX was loaded into the nuclear regions or the surrounding nuclear membrane. This demonstrated that the intracellular uptake of DOX was increased in a time-dependent manner and the HA-PHis micelles were able to effectively deliver DOX to the cytoplasm due to pH-responsive release. In addition, as the DS increased, the cellular fluorescence intensity of DOX became weaker in MCF-7 cells. After a 2 h incubation, HPHM-19 exhibited the highest nuclear fluorescence intensity compared with the other groups. However, HPHM-28, compared with HPHM-19, HPHM-22 and free DOX, exhibited the weakest fluorescence. This surprising result is consistent with that provided by cytotoxicity assays and further confirms that the carboxyl active sites of HA are intimately associated with CD44 receptor-mediated uptake.

The amount of cellular uptake was also assayed by flow cytometry. As shown in Fig. 6b and c, the increased cellular uptake in MCF-7 was also time dependent and HPHM-19 had a maximum value at each time point. Also, the cellular uptake of DOX in HPHM-19 was 1.2- and 2.6-fold higher than that in HPHM-22 and HPHM-28 in MCF-7 at 2 h. In particular, there was no significant difference between the intracellular uptake of HPHM-19 and that of HPHM-22 at 0.5 h ($P > 0.05$). However, a significant difference was found after incubation for 1 and 2 h ($P < 0.05$). This might be due to the fact that the degree of endocytosis of HPHM-19 and HPHM-22 was similar after a short period (e.g. 0.5 h) because of the slight difference in DS and the intracellular uptake increased with time. Although there was a time-dependent increase in the mean fluorescence intensity for each of the micelles after a 2 h incubation, the increase with HPHM-22 and HPHM-28 was less than that with HPHM-19. It might be that HA-PHis micelles with a high degree of substitution reduced the recognition sites of CD44 receptors, which could result in a low rate of uptake over time. In addition, the intracellular uptake of free DOX was lower than that of HPHM-19 and HPHM-22 ($P < 0.05$) and higher than that of HPHM-28 ($P < 0.05$). This is in line with the cytotoxicity assays and fluorescence microscopy results shown in Fig. 5 and Fig. 6a. All these results are in good agreement with the hypothesis that the carboxylic groups of HA are the active sites for combination with CD44 receptors overexpressed on the surface of MCF-7 cells.

In summary, the above results from qualitative and quantitative analysis indicate that the cellular uptake of the HA-PHis series of micelles is time dependent. The pH-responsive HA-PHis micelles significantly increase their accumulation in tumor sites by CD44 receptor-mediated endocytosis targeting and then the pH-triggered burst drug release provides rapid transport of DOX into the cytosol, which significantly increases the antitumor efficacy of DOX against MCF-7 cells. Furthermore, the DS of HA derivates has such an important influence on CD44 receptor-mediated endocytosis that the cellular uptake is reduced when the DS exceeds a certain critical value.

3.6. Cellular uptake route

A variety of forms of endocytosis have been shown to be involved in the cellular uptake of copolymer micelles [55]. To elucidate the potential cellular uptake pathways, the interaction between HPHM-19 and the cell membrane was investigated by treating cells with different chemical inhibitors of caveolae-mediated

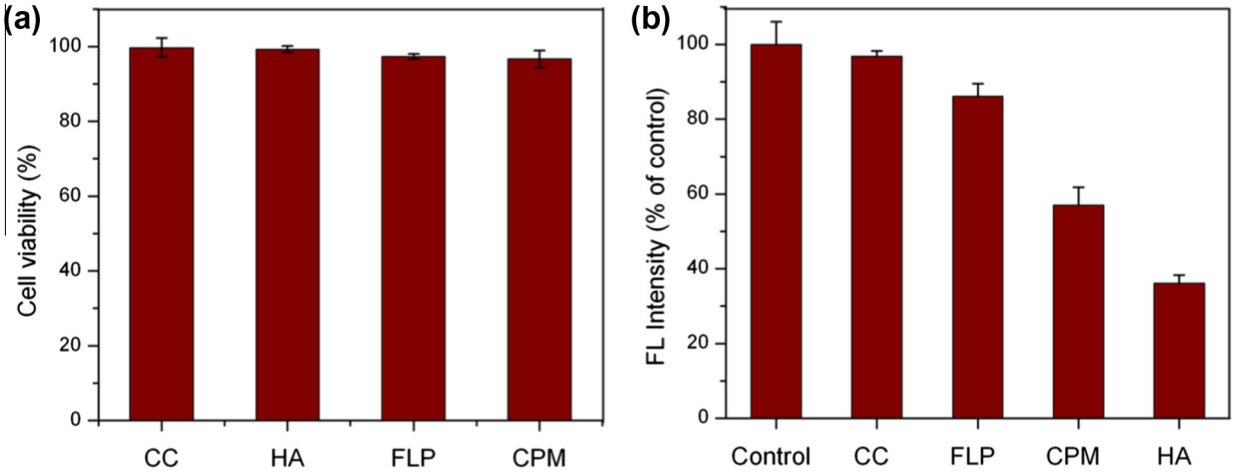

Fig. 7. (a) Viability of cells treated with different inhibitors and (b) effects of inhibitors on the internalization of HPHM-19 in MCF-7 cells ($n = 3$).

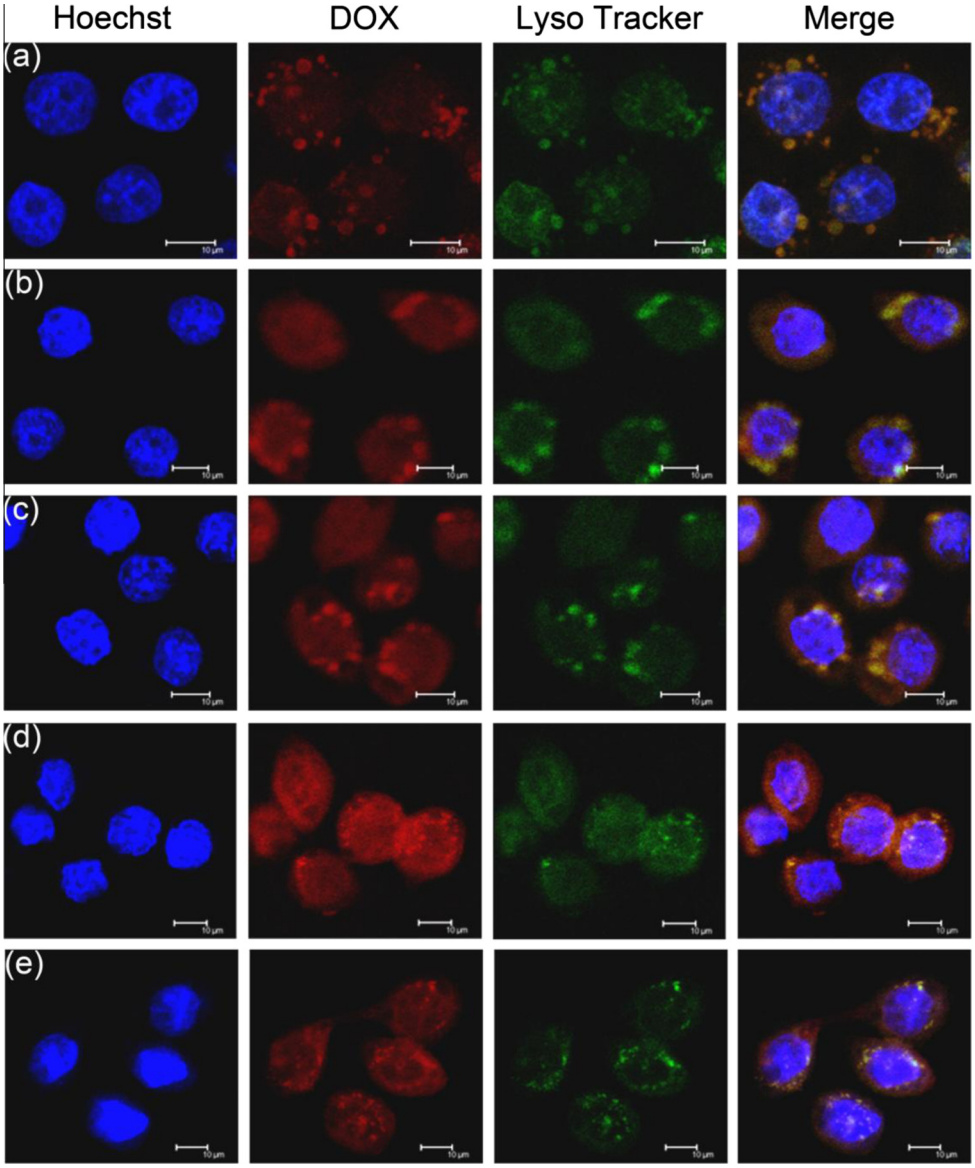

Fig. 8. LSCM images of the intracellular distribution of DOX. For each panel, images from left to right show cell nuclei stained by Hoechst 33342 (blue), DOX (red), lysosome stained by Lysotracker (green) and overlays of all images. MCF-7 cells were incubated with HPHM-19 for: (a) 10 min, (b) 30 min, (c) 60 min, (d) 120 min and (e) 120 min in the presence of chloroquine. The bar represents 10 μm.

endocytosis, clathrin-mediated endocytosis, macropinocytosis and receptor inhibitors. As shown in Fig. 7a, the concentration of each inhibitor used in cellular uptake did not significantly reduce the cell viability, showing that the inhibitors were nontoxic to the cells.

Fig. 7b shows the results of the internalization of HPHM-19 in the presence of various inhibitors; the counterparts in the absence of inhibitors were used as controls. Compared with the control group, the cellular uptake of micelles was reduced by 64% in the presence of HA ($P < 0.05$). It was suggested that CD44 receptors could be blocked by HA, resulting in the reduced fluorescence intensity of copolymer micelles. This indicates that the competitive binding of HA to CD44 receptors reduced the cellular uptake of HPHM-19 via CD44 receptor-mediated endocytosis. The effect of the macropinocytosis pathway on the uptake of micelles was evaluated using CC. Relative to the control, the reduction in internalization of micelles was 3% ($P > 0.05$), implying that macropinocytosis was not closely involved in the internalization of micelles. In contrast, in the presence of CPM and FLP (clathrin-mediated pathway inhibitor and caveolae-mediated pathway inhibitor, respectively), the cellular uptake of micelles was reduced by 43% and 14% ($P < 0.05$). These data suggest that the clathrin-mediated pathway plays a major role in the uptake of HA-PHis micelles while a minor fraction of the micelles could be internalized via caveolae-mediated endocytosis.

3.7. Intracellular release of DOX

The intracellular drug release behavior of HPHM-19 was evaluated by LSCM, as shown in Fig. 8. After incubation for 10 and 30 min, DOX was dispersed in the cytoplasm, showing a co-localization with green fluorescence of lysosomes, which produced a yellow fluorescence in merged images (Fig. 8a,b). This suggests that micelles are first localized in lysosomes after being taken up by cells. The red fluorescence was increased in the cytoplasm and some weak fluorescence was around the nuclei following a 60 min incubation (Fig. 8c). After a prolonged incubation (120 min), it was noted that strong DOX fluorescence was observed in the cytoplasm and nuclei while the yellow fluorescence was

gradually disappeared (Fig. 8d). This suggests that the HPHM-19 is rapidly disassembled under acid conditions in lysosomes and DOX is released into the cytoplasm and nuclei of cells. Interestingly, when the pH of the lysosome compartment was increased by treatment with chloroquine, almost no red fluorescence was observed in the nuclei (Fig. 8e), ensuring that the pH-responsive characteristics increased intracellular drug release from HA-PHis micelles.

4. Conclusions

pH-Responsive biodegradable HA-PHis copolymers with different DS were synthesized and a series of self-assembled micelles with pH-responsive properties were prepared for specific targeted delivery of DOX to HA receptor overexpressing cancer cells. In vitro studies showed that the micelles could release DOX in a pH-responsive manner and the blank micelles were nontoxic to MCF-7 cells. Furthermore, HPHM-19, based on the low DS of HA-PHis, exhibited high cytotoxicity, efficient internalization and rapid, pH-triggered drug release to achieve the highest intracellular drug concentration. Endocytosis inhibition studies revealed that HPHM-19 was internalized mainly via clathrin-mediated endocytosis and transported to lysosomes, where DOX was released from the micelles and finally penetrated into the nuclei. All of these results demonstrate that the HA-PHis copolymer is useful as a biocompatible, tumor-targeted and pH-responsive nanocarrier and is an attractive way to improve the intracellular delivery of hydrophobic anticancer drugs.

Acknowledgments

This work was supported by National Natural Science Foundation of China (No. 81173004, 81202473 and 81302719).

Appendix A. Figures with essential colour discrimination

Certain figures in this article, particularly Figs. 2–8 and Schemes S1 and S2, are difficult to interpret in black and white. The full colour images can be found in the on-line version, at http://dx.doi.org/10.1016/j.actbio.2013.12.025.

References

[1] Guan XW, Li YH, Jiao ZX, Chen J, Guo ZP, Tian HY, et al. A pH-sensitive charge-conversion system for doxorubicin delivery. Acta Biomater 2013;9:7672–8.
[2] Cheng Y, Hao J, Lee LA, Biewer MC, Wang Q, Stefan MC. Thermally controlled release of anticancer drug from self-assembled γ-substituted amphiphilic poly (ε-caprolactone) micellar nanoparticles. Biomacromolecules 2012;13:2163–73.
[3] Choi KY, Jeon EJ, Yoon HY, Lee BS, Na JH, Min KH, et al. Theranostic nanoparticles based on PEGylated hyaluronic acid for the diagnosis, therapy and monitoring of colon cancer. Biomaterials 2012;33:6186–93.
[4] Davis ME. Nanoparticle therapeutics: an emerging treatment modality for cancer. Nat Rev Drug Discov 2008;7:771–82.
[5] Wu Y, Chen W, Meng FH, Wang ZJ, Cheng R, Deng C, et al. Core-crosslinked pH-sensitive degradable micelles: a promising approach to resolve the extracellular stability versus intracellular drug release dilemma. J Control Release 2012;164:338–45.
[6] Torchilin V. Tumor delivery of macromolecular drugs based on the EPR effect. Adv Drug Deliver Rev 2011;63:131–5.
[7] Tao YH, Liu R, Chen MQ, Yang C, Liu XY. Cross-linked micelles of graftlike block copolymer bearing biodegradable ε-caprolactone branches: a novel delivery carrier for paclitaxel. J Mater Chem 2011;22:373–80.
[8] Mi Y, Liu Y, Feng SS. Formulation of docetaxel by folic acid-conjugated d-α-tocopheryl polyethylene glycol succinate 2000 (Vitamin E TPGS$_{2k}$) micelles for targeted and synergistic chemotherapy. Biomaterials 2011;32:4058–66.
[9] Cimini A, D'Angelo B, Das S, Gentile R, Benedetti E, Singh V, et al. Antibody-conjugated PEGylated cerium oxide nanoparticles for specific targeting of Aβ aggregates modulate neuronal survival pathways. Acta Biomater 2012;8:2056–67.
[10] Wang ZL, Xu B, Zhang L, Zhang JB, Ma TH, Zhang JB, et al. Folic acid-functionalized mesoporous silica nanospheres hybridized with AIE luminogens for targeted cancer cell imaging. Nanoscale 2013;5:2065–72.
[11] Yang L, Zhang XB, Ye M, Jiang JH, Yang RH, Fu T, et al. Aptamer-conjugated nanomaterials and their applications. Adv Drug Deliver Rev 2011;63:1361–70.
[12] Dohmen C, Edinger D, Fröhlich T, Schreiner L, Lächelt U, Troiber C, et al. Nanosized multifunctional polyplexes for receptor-mediated siRNA delivery. ACS Nano 2012;6:5198–208.
[13] Jing Y, Zhang L, Zhou J, Liu HP, Zhang Q. Efficient simultaneous tumor targeting delivery of all-trans retinoid acid and paclitaxel based on hyaluronic acid-based multifunctional nanocarrier. Mol Pharm 2013;10:1080–91.
[14] Camci-Unal G, Cuttica D, Annabi N, De Marchi D, Khademhosseini A. Synthesis and characterization of hybrid hyaluronic acid-gelatin hydrogels. Biomacromolecules 2013;14:1089–92.
[15] Jin YJ, Termsarasab U, Ko SH, Shim JS, Chong S, Chung SJ, et al. Hyaluronic acid derivative-based self-assembled nanoparticles for the treatment of melanoma. Pharm Res 2012;29:3443–54.
[16] Prestwich GD. Hyaluronic acid-based clinical biomaterials derived for cell and molecule delivery in regenerative medicine. J Control Release 2011;155:193–9.
[17] Choi KY, Yoon HY, Kim J-H, Bae SM, Park R-W, Kang YM, et al. Smart nanocarrier based on PEGylated hyaluronic acid for cancer therapy. ACS Nano 2011;5:8591–9.
[18] Cho HJ, Yoon HY, Koo H, Ko SH, Shim JS, Lee JH, et al. Self-assembled nanoparticles based on hyaluronic acid-ceramide (HA-CE) and Pluronic® for tumor-targeted delivery of docetaxel. Biomaterials 2011;32:7181–90.
[19] Yao J, Zhang L, Zhou JP, Liu HP, Zhang Q. Efficient simultaneous tumor targeting delivery of all-trans retinoid acid and paclitaxel based on hyaluronic acid-based multifunctional nanocarrier. Mol Pharm 2013;10:1080–91.
[20] Choi KY, Min KH, Na JH, Choi K, Kim K, Park JH, et al. Self-assembled hyaluronic acid nanoparticles as a potential drug carrier for cancer therapy: synthesis, characterization, and *in vivo* biodistribution. J Mater Chem 2009;19:4102–7.
[21] Cajot S, Van Butsele K, Paillard A, Passirani C, Garcion E, Benoit J, et al. Smart nanocarriers for pH-triggered targeting and release of hydrophobic drugs. Acta Biomater 2012;8:4215–23.
[22] Tang DL, Song F, Chen C, Wang XL, Wang YZ. A pH-responsive chitosan-b-poly (p-dioxanone) nanocarrier: formation and efficient antitumor drug delivery. Nanotechnology 2013;24:145101.
[23] Dadsetan M, Efua Taylor K, Yong C, Bajzer Ž, Lu L, Yaszemski MJ. Controlled release of doxorubicin from pH-responsive microgels. Acta Biomater 2013;9:5438–46.
[24] Li J, Huo MR, Wang J, Zhou JP, Mohammad JM, Zhang YL, et al. Redox-sensitive micelles self-assembled from amphiphilic hyaluronic acid-deoxycholic acid conjugates for targeted intracellular delivery of paclitaxel. Biomaterials 2012;33:2310–20.
[25] Felber AE, Dufresne MH, Leroux JC. PH-sensitive vesicles, polymeric micelles, and nanospheres prepared with polycarboxylates. Adv Drug Deliver Rev 2012;64:979–92.
[26] Fan JQ, Zeng F, Wu SZ, Wang XD. Polymer micelle with pH-triggered hydrophobic–hydrophilic transition and de-cross-linking process in the core and its application for targeted anticancer drug delivery. Biomacromolecules 2012;13:4126–37.
[27] Yang YQ, Zhao B, Li ZD, Lin WJ, Zhang CY, Guo XD, et al. PH-sensitive micelles self-assembled from multi-arm star triblock co-polymers poly(ε-caprolactone)-b-poly(2-(diethylamino)ethyl methacrylate)-b-poly(poly (ethylene glycol) methyl ether methacrylate) for controlled anticancer drug delivery. Acta Biomater 2013;9:7679–90.
[28] Lee YJ, Kang HC, Hu J, Nichols JW, Jeon YS, Bae YH. PH-sensitive polymeric micelle-based pH probe for detecting and imaging acidic biological environments. Biomacromolecules 2012;13:2945–51.
[29] Yin H, Kang HC, Huh KM, Bae YH. Biocompatible, pH-sensitive AB2 miktoarm polymer-based polymersomes: preparation, characterization, and acidic pH-activated nanostructural transformation. J Mater Chem 2012;22:19168–78.
[30] Lee ES, Shin HJ, Na K, Bae YH. Poly (l-histidine)–PEG block copolymer micelles and pH-induced destabilization. J Control Release 2003;90:363–74.
[31] Casey JR, Grinstein S, Orlowski J. Sensors and regulators of intracellular pH. Nat Rev Mol Cell Biol 2009;11:50–61.
[32] Hu XL, Li H, Luo SZ, Liu T, Jiang YY, Liu SY. Thiol and pH dual-responsive dynamic covalent shell cross-linked micelles for triggered release of chemotherapeutic drugs. Polym Chem 2013;4:695–706.
[33] Harada H, Takahashi M. CD44-dependent intracellular and extracellular catabolism of hyaluronic acid by hyaluronidase-1 and-2. J Biol Chem 2007;282:5597–607.
[34] Ouasti S, Kingham PJ, Terenghi G, Tirelli N. The CD44/integrins interplay and the significance of receptor binding and re-presentation in the uptake of RGD-functionalized hyaluronic acid. Biomaterials 2012;33:1120–34.
[35] Banerji S, Wright AJ, Noble M, Mahoney DJ, Campbell ID, Day AJ, et al. Structures of the CD44–hyaluronan complex provide insight into a fundamental carbohydrate-protein interaction. Nat Struct Mol Biol 2007;14:234–9.
[36] Liu YH, Sun J, Cao W, Yang JH, Lian H, Li X, et al. Dual targeting folate-conjugated hyaluronic acid polymeric micelles for paclitaxel delivery. Int J Pharm 2011;421:160–9.

[37] Bailly N, Thomas M, Klumperman B. Poly (N-vinylpyrrolidone)-block-poly (vinyl acetate) as a drug delivery vehicle for hydrophobic drugs. Biomacromolecules 2012;13:4109–17.
[38] Seo K, Kim D. PH-dependent hemolysis of biocompatible imidazole-grafted polyaspartamide derivatives. Acta Biomater 2010;6:2157–64.
[39] Choi WI, Yoon KC, Im SK, Kim YH, Yuk SH, Tae G. Remarkably enhanced stability and function of core/shell nanoparticles composed of a lecithin core and a pluronic shell layer by photo-crosslinking the shell layer: *in vitro* and *in vivo* study. Acta Biomater 2010;6:2666–73.
[40] Cai GQ, Zhang HW, Liu P, Wang LQ, Jiang HL. Triggered disassembly of hierarchically assembled onion-like micelles into the pristine core–shell micelles via a small change in pH. Acta Biomater 2011;7:3729–37.
[41] Peng SF, Tseng MT, Ho YC, Wei MC, Liao ZX, Sung HW. Mechanisms of cellular uptake and intracellular trafficking with chitosan/DNA/poly (γ-glutamic acid) complexes as a gene delivery vector. Biomaterials 2011;32:239–48.
[42] Zheng M, Zhong ZH, Zhou L, Meng FH, Peng R, Zhong ZY. Poly (ethylene oxide) grafted with short polyethylenimine gives DNA polyplexes with superior colloidal stability, low cytotoxicity, and potent *in vitro* gene transfection under serum conditions. Biomacromolecules 2012;13:881–8.
[43] Huo M, Zhang Y, Zhou JP, Zou AF, Yu D, Wu YP, et al. Synthesis and characterization of low-toxic amphiphilic chitosan derivatives and their application as micelle carrier for antitumor drug. Int J Pharm 2010;394:162–73.
[44] Lo C-L, Huang C-K, Lin K-M, Hsiue G-H. Mixed micelles formed from graft and diblock copolymers for application in intracellular drug delivery. Biomaterials 2007;28:1225–35.
[45] Chen CY, Kim TH, Wu W-C, Huang CM, Wei H, Mount CW, et al. PH-dependent, thermosensitive polymeric nanocarriers for drug delivery to solid tumors. Biomaterials 2013;34:4501–9.
[46] Li Y, Li H, Wei M, Lu J, Jin L. pH-responsive composite based on prednisone-block copolymer micelle intercalated inorganic layered matrix: Structure and *in vitro* drug release. Chem Eng J 2009;151:359–66.
[47] Wischke C, Schwendeman SP. Principles of encapsulating hydrophobic drugs in PLA/PLGA microparticles. Int J Pharm 2008;364:298–327.
[48] Young CR, Dietzsch C, Cerea M, Farrell T, Fegely KA, Rajabi-Siahboomi A, et al. Physicochemical characterization and mechanisms of release of theophylline from melt-extruded dosage forms based on a methacrylic acid copolymer. Int J Pharm 2005;301:112–20.
[49] Lee ES, Oh KT, Kim D, Youn YS, Bae YH. Tumor pH-responsive flower-like micelles of poly (L-lactic acid)-b-poly (ethylene glycol)-b-poly (L-histidine). J Control Release 2007;123:19–26.
[50] Fredenberg S, Wahlgren M, Reslow M, Axelsson A. The mechanisms of drug release in poly (lactic-co-glycolic acid)-based drug delivery systems – a review. Int J Pharm 2011;415:34–52.
[51] Luo ZL, Jiang JW. PH-sensitive drug loading/releasing in amphiphilic copolymer PAE-PEG: integrating molecular dynamics and dissipative particle dynamics simulations. J Control Release 2012;162:185–93.
[52] Johnson RP, Jeong YI, John JV, Chung C-W, Kang DH, Selvaraj M, et al. Dual stimuli-responsive poly (N-isopropylacrylamide)-b-poly (L-histidine) chimeric materials for the controlled delivery of doxorubicin into liver carcinoma. Biomacromolecules 2013;14:1434–43.
[53] Yin HH, Lee ES, Kim D, Lee KH, Oh KT, Bae YH. Physicochemical characteristics of pH-sensitive poly(L-Histidine)-b-poly(ethylene glycol)/poly(L-Lactide)-b-poly(ethylene glycol) mixed micelles. J Control Release 2008;126:130–8.
[54] Liu R, Li D, He B, Xu XH, Sheng MM, Lai Y, et al. Anti-tumor drug delivery of pH-sensitive poly(ethylene glycol)-poly(L-histidine-)-poly(L-lactide) nanoparticles. J Control Release 2011;152:49–56.
[55] Sokolova V, Kozlova D, Knuschke T, Buer J, Westendorf AM, Epple M. Mechanism of the uptake of cationic and anionic calcium phosphate nanoparticles by cells. Acta Biomater 2013;9:7527–35.